SIN-CHN SCIENTIFIC PRESS PTE.LTD.

Molecular & Cellular Biomechanics 2025, 22(1), 662.
https://doi.org/10.62617/mcb662

Article

Protective effects of a combination of salvia miltiorrhiza bunge and astragalus membranaceus bunge against concanavalin A-induced liver injury in rats: A biomechanical perspective

Tong Guan[1], Jian Fan[2], Feng Guan[1], Yanhong Wang[1,*]

[1] School of Pharmacy, Heilongjiang University of Chinese Medicine, Harbin 150040, China
[2] The State Key Laboratory of Functions and Applications of Medicinal Plants, Guizhou Medical University, Guiyang 550014, China
*** Corresponding author:** Yanhong Wang, wang.yanhong@163.com

CITATION

Guan, T, Fan J, Guan F, Wang Y. Protective effects of a combination of salvia miltiorrhiza bunge and astragalus membranaceus bunge against concanavalin A-induced liver injury in rats: A biomechanical perspective. Molecular & Cellular Biomechanics. 2025; 22(1): 662. https://doi.org/10.62617/mcb662

ARTICLE INFO

Received: 30 October 2024
Accepted: 13 November 2024
Available online: 10 January 2025

Abstract: Immune liver injury is a special type of chronic liver disease caused by immune dysfunction in the body. Salvia Miltiorrhiza (Danshen) and Astragalus membranaceus (Huangqi) have shown a synergistic effect in treating liver diseases in clinical settings. Nevertheless, the ideal combination ratio, dosage, and underlying mechanism of action of them remain uncertain. This research aimed to explore the biomechanical and immunological mechanisms of the combined use of Danshen and Huangqi in the treatment of liver injury, Which points to the regulation of lymphocyte biomechanics. To induce liver injury in rats, we administered Concanavalin A (ConA) via the tail vein. By observing liver indicators, serum biochemical indicators and liver tissue pathological changes in rats, the optimal ratio and dosage of the combination of "Danshen-Huangqi" was determined. Flow cytometry was used to analyze T lymphocyte subsets in rat peripheral blood. ELISA was performed to measure serum cytokine levels. RT-PCR was conducted to quantify specific transcription factors in rat aged 6–8 weeks liver tissue. Immunohistochemistry was utilized to evaluate the expression of apoptosis-related genes in rat liver tissue. The findings demonstrated that "Danshen-Huangqi" exerts bidirectional regulation on T lymphocyte subsets., influencing their biomechanical properties, such as cell stiffness and migratory behavior. The combination modulates the secretion of Th1, Th2, Th17, and Treg cytokines and specific transcription factors, thus rectifying the imbalance of Th1/Th2 and Th17/Treg ($P < 0.05$) lymphocyte subsets, but also inhibits atypical apoptosis of liver lymphocytes by controlling the expression of apoptosis-related genes in the rat liver with liver injury through the death receptor pathway and mitochondrial pathway. The biomechanical interactions of herbal remedies is to have a full effect on the protein molecules of target cells. Thus, the combination of Danshen and Huangqi may be a promising drug pair in improving liver injury. Compared with existing treatment options, this study is more mild and can be applied more widely in different populations.

Keywords: biomechanics; salvia miltiorrhiza bunge; astragalus membranaceus (Fisch.) bunge; concanavalin A; liver injury; T lymphocyte

1. Introduction

The liver plays a crucial role as an immune organ within the human body and has functions such as regulating protein synthesis, secreting biochemical enzymes, and detoxifying foreign substances. When a large number of viruses invade the body, various inflammatory cells accumulate in the liver, prompting the immune system to produce excessive immune response, leading to liver cell damage [1,2]. Liver injury is frequently induced by a variety of factors, such as immune dysfunction, long-term alcoholism, viral infections and drug effects [3]. It has increasingly become an

"invisible killer" threatening human health. Therefore, effective prevention of liver injury is extremely important. The animal model of immune liver injury induced by Con A has high similarity with human immune liver injury patients in histological and serological characteristics [4,5]. The pathogenesis primarily entails the activation and recruitment of T cells within the liver, integrating innate and adaptive immunity to generate a diverse array of effector cells and molecules. This process results in significant inflammatory cell infiltration in liver tissue, leading to concurrent damage and necrosis. Its main characteristics are elevated serum aminotransferases, release of inflammatory cytokines, and abnormal hepatocyte apoptosis. Among them, ALT, AST, and LDH are the liver function indicators most sensitive to liver injury [6]. Moreover, liver injury induced by ConA engages critical factors encompassing T lymphocyte subsets, specifically CD3+, CD4+, and CD8+, along with cytokines related to Th1, Th2, Th17, and Treg. Furthermore, transcription factors such as T-bet, GATA-3, RORγt, and Foxp3, which are specific to various T cell subtypes, as well as genes associated with apoptosis such as Fas, FasL, Bax, and Bcl-2, play pivotal roles in this process [7–13]. Prior investigations have demonstrated that the injection of Con A into the tail vein of mice can result in the release of numerous cytokines, including TNF-α, IFN-γ, and TGF-β, among others, as well as inflammatory mediators, ultimately leading to the development of liver injury [14]. It is noteworthy that IL-8 not only stimulates the secretion of TNF-α but also enhances the expression of FasL on hepatocytes' surface, thus contributing to hepatocyte damage [15].

Traditional Chinese medicine is known for its wide range of indications, targeting multiple pathways and various targets. Numerous drugs and active ingredients have demonstrated hepatoprotective effects, acting on multiple stages of liver damage. Danshen and Huangqi are traditional Chinese medicines that can be used for health food published by the China Health Commission. Both of them have hepatoprotective effects. The combination of them is the main drug pair for clinical prevention and treatment of hepatitis and liver cirrhosis, with definite curative effect. Astragaloside IV and salvianolic acid B are the key effective components of Danshen and Huangqi respectively [16–18]. Research has indicated that both of these components contain gallic acid, which has been proven to have a beneficial effect in reducing the activity of the hepatitis B virus [19]. Previous research has validated that the combination of astragaloside IV and salvianolic acid B has a synergistic protective impact on peroxide-induced liver cell damage [20]. Nonetheless, there is a lack of study on the safeguarding influence of Danshen combined with Huangqi against concanavalin A-induced liver injury both domestically and internationally. The purpose of this study is to develop "Danshen-Huangqi" into a kind of Chinese herbal medicine health food with auxiliary protective effect on liver injury, and to further study the potential protective mechanism of "Danshen-Huangqi" on liver injury from the perspectives of T lymphocyte subsets, cytokines, specific transcription factors and apoptosis-related genes by using the liver injury animal model induced by concanavalin A suitable for immunological research.

2. Material and methods

2.1. Animals

Female SD rats (aged 6–8 weeks; 180 ± 20 g) were purchased from Drug Safety Evaluation Center of Heilongjiang University of Chinese Medicine (Harbin, China). Before entering the experimental stage, the rats adapted in advance for one week, and were free to drink and eat during the adaptation period. The experimental environment maintained a temperature of 25 °C ± 2 °C and a relative humidity of 60 % ± 5 %. The Animal Ethics Committee of Heilongjiang University of Chinese Medicine approved the experimental protocol, which adhered to the guidelines established by the National Institute of Health and Nutrition for the Care and Use of Laboratory Animals.

2.2. Reagents and herbal materials

ConA was acquired from Sigma-Aldrich (20190624, USA). The aminotransferase of aspartate (AST), aminotransferase of alanine (ALT), and lactate dehydrogenase (LDH) kits, as well as IL-2, IL-4, IL-6, IL-10, IL-17, IL-21, TNF-α, TGF-β, and IFN-γ, were procured from Nanjing Jiancheng Institute of Bioengineering (Nanjing, China). Anti-Rat CD3 PITC, Anti-Rat CD4 PerCP, and Anti-Rat CD8a PE were obtained from Becton, Dickinson & Company (USA). Fas, FasL, Bax, and Bcl-2 were purchased from Wanlei Biotechnology Co., Ltd (Nanjing, China). Bifendate dropping pills were procured from Beijing Xiehe Pharmaceutical Factory (Beijing, China). Salvia Miltiorrhiza Bunge and Astragalus membranaceus (Fisch.) Bunge were both acquired from Harbin Sankeshu Medicinal Material Market (Harbin, China).

2.3. Preparation of test drugs

Salvia Miltiorrhiza Bunge freeze-dried powder: The appropriate amount of Salvia Miltiorrhiza Bunge was weighed, crushed, immersed in twelve-fold distilled water and allowed to soak for a duration of 1.5 h, refluxed at 80 ℃ for 2 times, 2 h/time, concentrated under reduced pressure, and freeze-dried by freeze-drying machine. Astragalus membranaceus (Fisch.) Bunge freeze-dried powder: The appropriate amount of Astragalus membranaceus (Fisch.) Bunge was weighed, crushed, immersed in twelve-fold distilled water and allowed to soak for a duration of 2 h, heated and refluxed for 3 times, 1.5 h/time, concentrated under reduced pressure, and freeze-dried by freeze-drying machine.

2.4. Drug treatment and ConA-induced liver injury model in mice

The optimal compatibility ratio grouping of “Danshen-Huangqi”: 120 SD rats were randomly divided into 10 groups: blank group (K group), model group (M group), positive group (Y group), Danshen group (D group), Huangqi group (H group), Danshen-Huangqi 1:0.5 group (D-H1:0.5 group), Danshen-Huangqi 1:1 group (D-H1:1 group), Danshen-Huangqi 1:2 group (D-H1:2 group), Danshen-Huangqi 1:3 group (D-H1:3 group) and Danshen-Huangqi 1:4 group (D-H1:4 group), with 12 rats in each group.

The optimal dosage of grouping of “Danshen-Huangqi”: 72 SD rats were randomly divided into 6 groups: K group, M group, Y group, D-H1: 2 low dose group, D-H1: 2 middle dose group and D-H1: 2 high dose group, with 12 rats in each group.

The Y group was administered bifendate dropping pills at a dosage of 0.94 mg/kg. The D group received Danshen freeze-dried powder at a dosage of 0.5 g/kg, while the

H group received Huangqi freeze-dried powder at a dosage of 1.0 g/kg. The proportions of Danshen-Huangqi freeze-dried powder varied among the D-H groups, specifically: 0.5,0.25 g/kg (1:0.5); 0.5, 0.5 g/kg (1:1); 0.5, 1.0 g/kg (1:2); 0.5, 1.5 g/kg (1:3); 0.5, 2.0 g/kg (1:4). Furthermore, The D-H low-dose group received 0.1, 0.2 g/kg. The D-H medium-dose group received 0.5, 1.0 g/kg. The D-H high-dose group received 1.0, 2.0 g/kg.

Grouping of experimental animals in four experimental methods (T lymphocyte subsets were detected by flow cytometry, cytokines by ELISA, specific transcription factors by RT-PCR and apoptosis-related genes by immunohistochemistry): 60 SD rats were randomly divided into 5 groups: K group, M group, D group, H group, D-H group, with 12 rats in each group. The D group received Danshen freeze-dried powder at a dosage of 0.5 g/kg, while the H group received Huangqi freeze-dried powder at a dosage of 1.0 g/kg. The D-H group was given Danshen-Huangqi freeze-dried powder (0.5, 1.0 g/kg). Both the K Group and M Group were administered distilled water. Gavage administration was conducted continuously for a duration of 30 days, once per day.

Seven h after the last gastric administration, rats from the K group were injected with physiological saline (2 mL/kg) via the tail vein, while rats from the other groups received an injection of Con A (20 mg/kg) through the tail vein.

2.5. Determination of the optimal compatibility ratio and dosage of "D-H"

After instilling Con A or normal saline solution into the tail vein of rats for a duration of 12 h, the rats' weights were recorded. Blood were taken from the abdominal aorta and then subjected to centrifugation at a temperature of 4 ℃ and a rotational speed of 3500 r/min for a duration of 15 min. Subsequently, the resulting supernatant was carefully stored at a temperature of −80 ℃. A transaminase kit was utilized to analyze the levels of AST, ALT, and LDH in the rat serum, following the manufacturer's instructions from Nanjing Jiancheng Biotechnology Institute in China. To analyze the impact of different "Danshen-Huangqi" dosages on the liver index (liver weight/body weight) of rats, the entire liver was excised and weighed. The left lobe of the liver was subsequently immersed in a neutral formaldehyde solution, underwent a series of procedures including dehydration, transparency, wax soaking, embedding, fishing, spreading, and drying. Subsequently, the specimen was stained with HE. Finally, an analysis of the hepatocytes' pathological alterations was conducted using a light microscope.

2.6. Flow cytometric analysis

Using 200 μL of peripheral blood and mixing it with 3 mL of erythrocyte lysate, allow for 4 min incubation at room temperature. Subsequently, introduce 10 mL of cell staining buffer and centrifuge the mixture at 3500 r/min for 5 min. Eliminate the supernatant and employ the cell staining buffer to regulate the cell concentration to 1×10^7/mL, thereby creating a peripheral blood sample. The samples were added with FITC-$CD3^+$, PerCP-$CD4^+$ and PE-$CD8^+$ antibodies, respectively. Mix well, incubation for 30 min, 4 ℃, away from light, cell staining buffer 5 mL, centrifugation 5 min,

3500 r/min, discard the supernatant, cell staining buffer 0.5 mL was used for FACS detection and analysis.

2.7. Cytokine assay

Following the manufacturer's instructions, the enzyme-linked immunosorbent assay kit (Nanjing Jiancheng Bio-Engineering Institute, Nanjing, China) was employed to assess the serum concentrations of IL-2, IL-4, IL-6, IL-10, IL-17, IL-21, IFN-γ, TNF-α, and TGF-β in rats after a 12-h duration of injecting Con A or normal saline into the tail vein.

2.8. RNA extraction and real-time PCR

The liver tissue preserved in liquid nitrogen was used to isolate total RNA through the utilization of Trizol reagent (Thermo Fisher Scientific, USA). Reverse transcription was performed with ABI StepOne PULS fluorescence quantitative PCR (Foster, California, USA) to synthesize cDNA from total RNA, following the guidelines provided by the manufacturer. The calculation of the Ct value for each sample was performed using the Taq-Man SDS software, while the expression level of the target gene was represented as $2^{-\triangle\triangle Ct}$. Gene expression was detected by using SybrGreen qPCR master mixture and qPCR amplification was performed under the subsequent conditions: pre-denaturation at 95 °C for 3 min, 5 s at 95 °Cs, and 45 cycles of dena-turation at 60 °C for 30 s. The expression levels of every gene were standardized to the housekeeping gene β-actin, and the outcomes were presented as multiple alterations relative to the control. The primer sequence of the target gene is as follows: T-bet forward primer 5' GCCGTTTCTACCCTGACCTT 3' and reverse primer 5' GCTCACTGCTCGGAACTCTGT 3'; GATA-3 forward primer 5' ATTACCACCTATCCGCCCTAT 3' and reverse primer 5' CGGTTCTGCCCATTCATTT 3'; RoRγt forward primer 5' TCCACTCACCAGCCTTTCC 3' and reverse primer 5' GATTTATCCCCGATGTTTGTCT 3'; Foxp3 forward primer 5' GACAGTTTCCCACAAGCCAG 3' and reverse primer 5' TGGTGAAGTGGACTGACAGA 3'.

2.9. Immunohistochemical staining

The liver's left lateral lobe was prepared for analysis by fixing it in a neutral formaldehyde solution. After that, it underwent a series of routine procedures including dehydration, transparency, wax immersion, embedding, fishing, spreading, and drying. Subsequently, it was stained using the PV two-step immunohistochemical method, following the instructions provided in the kit (Wanke Biotechnology Co., Ltd., Shenyang, China). We utilized the Image-pro plus 6.0 pathological image analysis system to quantitatively assess the levels of positive expression of apoptosis-related genes, namely Fas, FasL, Bax, and Bcl-2. The relative expression of these genes was represented by the integrated optical density (IOD = positive area× average optical density).

2.10. Statistical analysis

IBM SPSS Statistics 25 was used for the statistical analysis. Experimental data outcomes are expressed using the mean ± standard deviation. The indication of significance difference is $P < 0.05$, while extremely significant difference is represented by $P < 0.01$. Variance homogeneity analysis is conducted using LSD, whereas variance heterogeneity analysis is performed using Dunnett's method.

3. Results

3.1. Determination of the optimal compatibility ratio of "Danshen-Huangqi"

3.1.1. Effects of different ratios on liver index in rats with liver injury

Based on the findings, it was observed that the liver index of rats in the M group exhibited a significantly higher value compared to the K group. All groups experienced a significant decrease in the liver index of rats when compared to the M group. In contrast to the Y group, the liver index of rats in the D-H 1:2 group displayed an increase, although the disparity was not deemed significant (**Figure 1**).

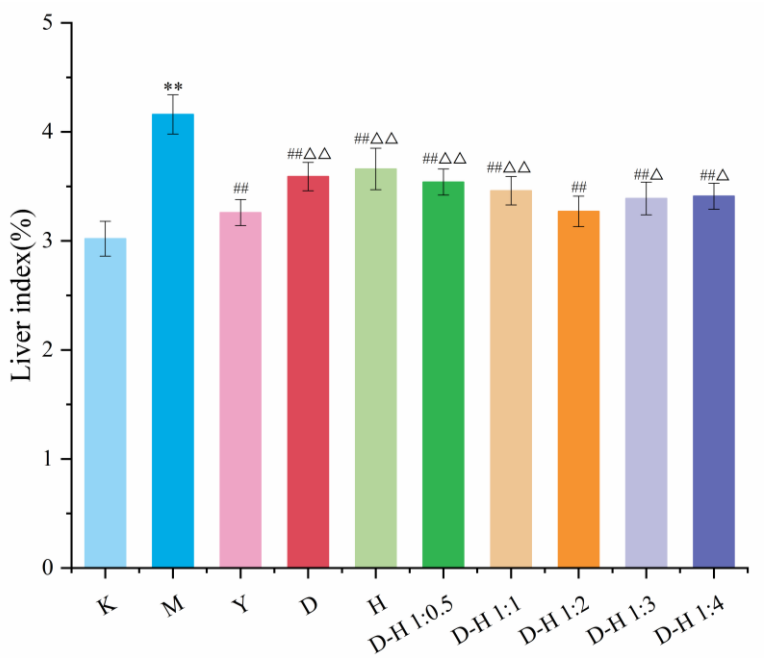

Figure 1. The effect of different ratio of herb pair on liver index of rats ($\bar{x} \pm s$, n = 12, %).

(Compared with group *K*, $^{**}P < 0.01$; Compared with group M, $^{\#\#}P < 0.01$; Compared with group *Y*, $^{\triangle}P < 0.05$, $^{\triangle\triangle}P < 0.01$.)

3.1.2. Effects of different ratios on biochemical indicators in rats with liver injury

The findings indicated that the serum levels of AST, ALT, and LDH in the M group were considerably elevated compared to those in the K group. Conversely, all groups exhibited notable reductions in the serum levels of AST, ALT, and LDH compared to the M group. The D-H 1:2 group displayed a substantial increase in the

serum levels of AST compared to the Y group, while the D-H 1:3 group exhibited significant increases in both ALT and LDH levels compared to the Y group (**Figure 2)**.

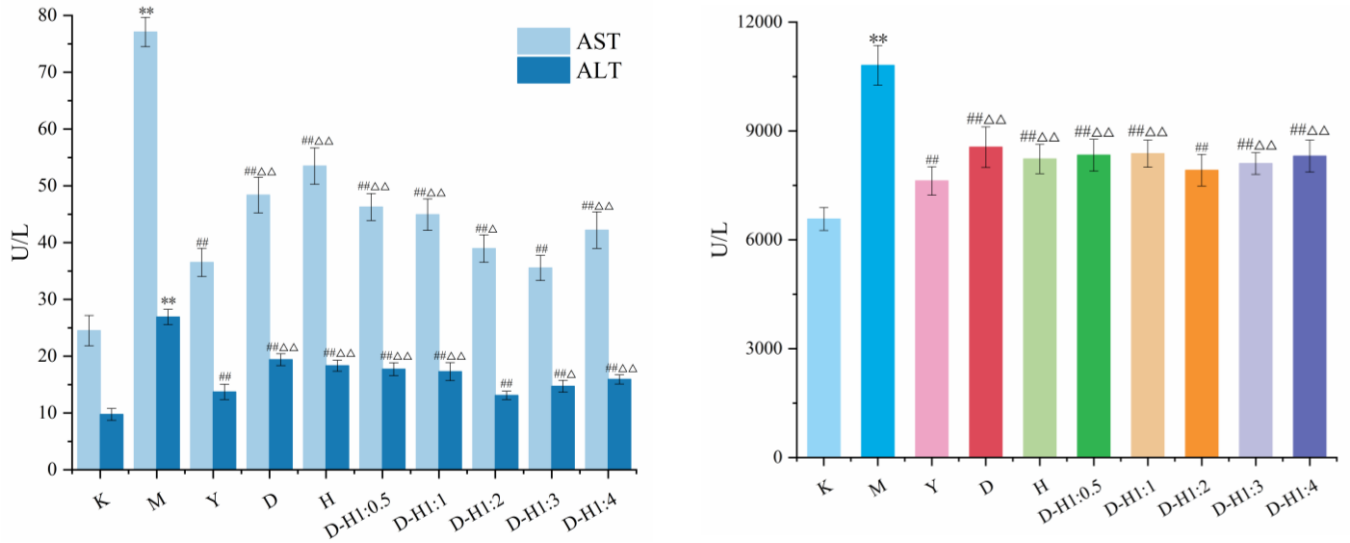

(A) **(B)**

Figure 2. The effect of different ratio of herb pair on the levels of AST, ALT **(A)** and LDH **(B)** in serum of rats ($\bar{x} \pm s$, n = 12, U/L).

(Compared with group *K*, $^{**}P < 0.01$; Compared with group *M*, $^{\#\#}P < 0.01$; Compared with group *Y*, $^{\triangle}P < 0.05$, $^{\triangle\triangle}P < 0.01$.)

3.1.3. Effects of different ratios on liver morphology in rats with liver injury

According to the findings, it was observed that K group exhibited a distinct and well-defined hepatic lobule structure, devoid of any hepatocyte necrosis or presence of macrophages. Conversely, when compared to the K group, the hepatic portal region of rats in the M group demonstrated a significant influx of inflammatory cells, elevated fibrous tissue, focal necrosis, and hepatic sinus congestion. Subsequently, in comparison to the M group, an improvement was observed in liver cell necrosis and inflammatory cell infiltration in rats from each treatment group, particularly in the Y group, D-H 1:2 group and D-H 1:3 group (**Figure 3**).

Comprehensive evaluation, “Danshen-Huangqi” had better intervention effect on liver injury at a ratio of 1: 2.

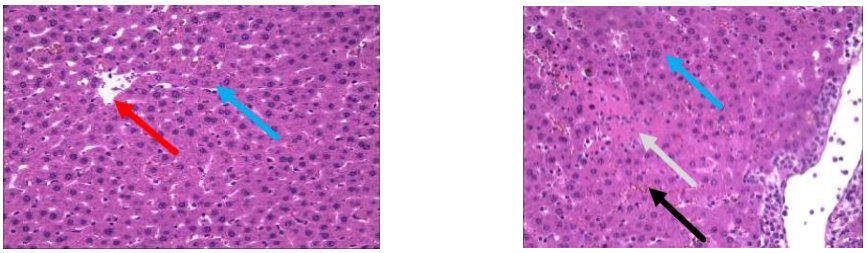

(A) **(B)**

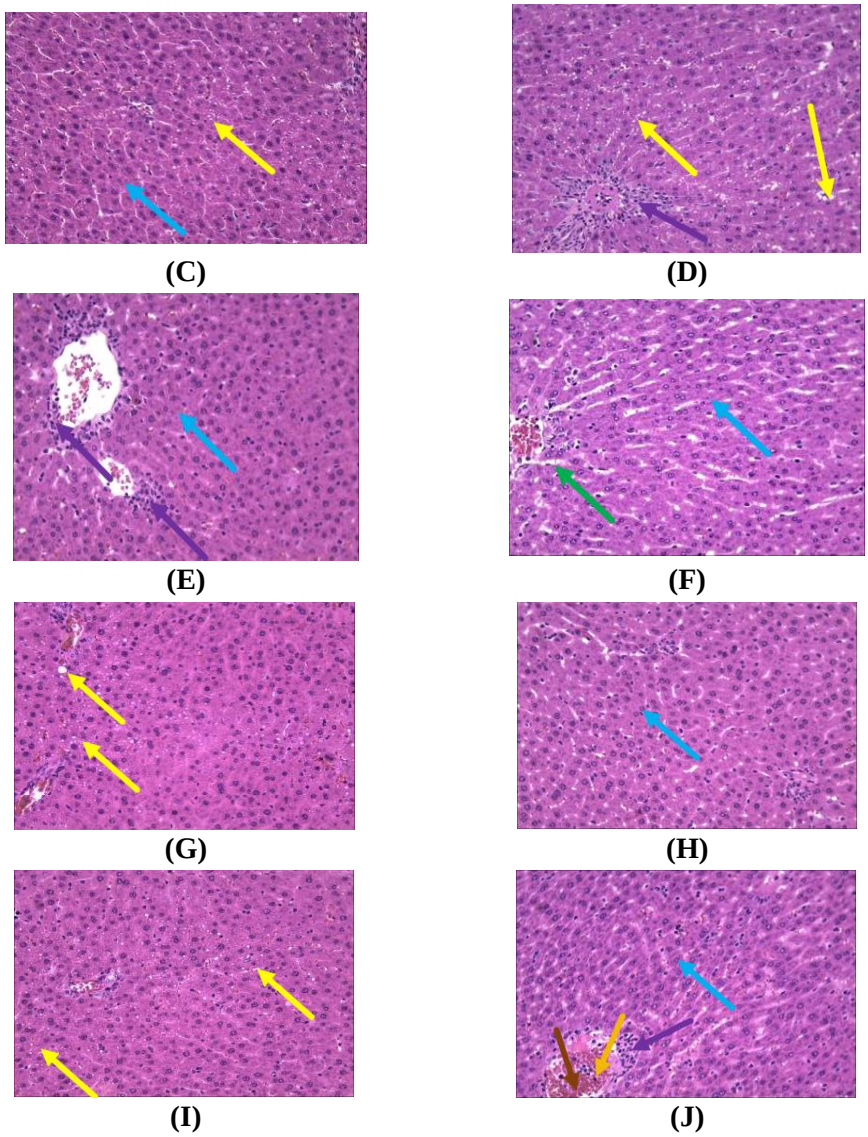

Figure 3. The effect of different ratio of herb pair on liver morphology of rats (400×). (Red arrow: central vein; Blue arrow: liver cells; Yellow arrow: hepatocyte steatosis, small vacuoles visible in the cytoplasm; Green arrow: slight expansion of hepatic sinus; Black arrow: Hepatic sinus congestion; Brown arrow: venous congestion; Purple arrow: perivascular lymphocyte infiltration; Grey arrow: liver cell necrosis, nuclear pyknosis, cytoplasm showed eosinophilic homogeneous.). **(A)**: K group; **(B)**: M group; **(C)**: Y group; **(D)**: D group; **(E)**: H group; **(F)**: D-H 1:0.5 group; **(G)**: D-H 1:1 group; **(H)**: D-H 1:2 group; **(I)**: D-H 1:3 group; **(J)**: D-H 1:4 group.

3.2. Determination of the optimal dosage of "Danshen-Huangqi"

3.2.1. Effects of different doses on liver index in rats with liver injury

The research findings indicated that the liver index of rats in the M group displayed a significant increase in comparison to the K group. Each administration group, in contrast to the M group, exhibited a noteworthy reduction in the liver index of rats. In comparison to the Y group, the liver index of rats in the low-dose D-H 1:2 group demonstrated a significant increase (**Figure 4**).

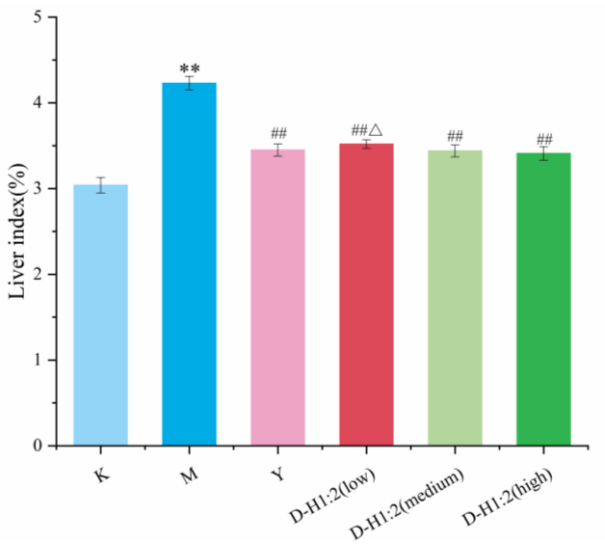

Figure 4. The effect of different doses of herb pair on liver index of rats ($\bar{x} \pm s$, n = 12, %).

(Compared with group K, $^{**}P < 0.01$; Compared with group M, $^{\#\#}P < 0.01$; Compared with group Y, $^{\triangle}P < 0.05$, $^{\triangle\triangle}P < 0.01$.)

3.2.2. Effects of different doses on biochemical indicators in rats with liver injury

The findings indicated that in comparison to the K group, the M group exhibited noticeably elevated serum levels of AST, ALT and LDH. Additionally, there was a significant decrease in the serum levels of AST, ALT, and LDH in each group when compared to the M group. Furthermore, when compared to the Y group, the serum levels of AST, LDH and ALT were significantly elevated in the D-H 1:2 low-dose group of rats (**Figure 5**).

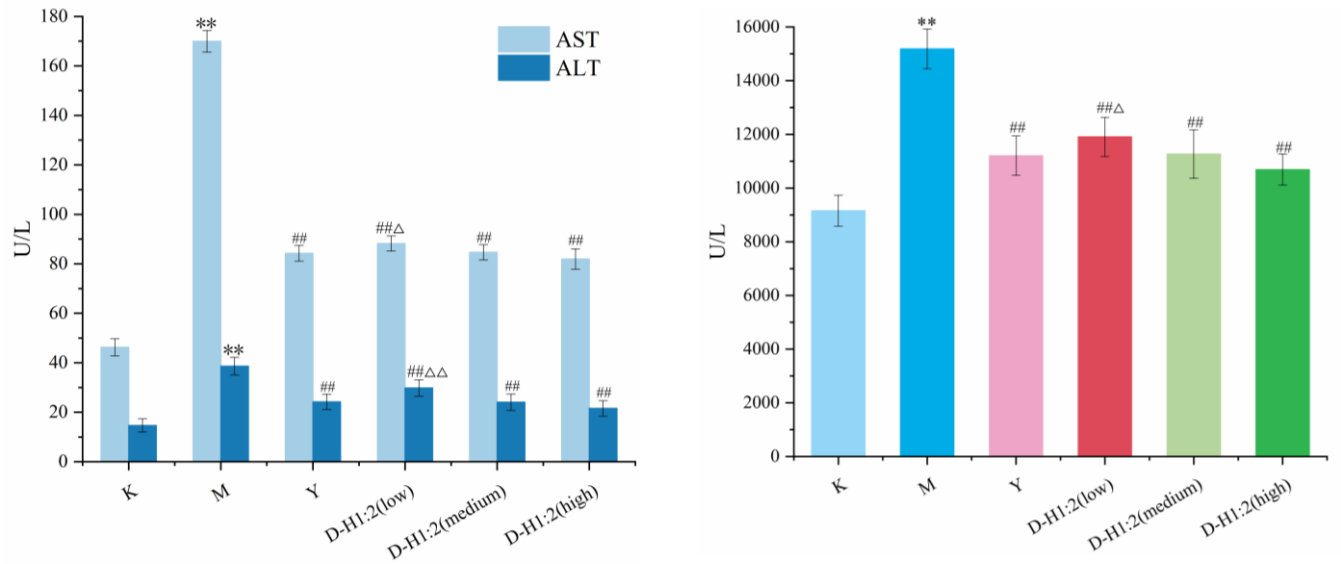

(**A**) (**B**)

Figure 5. The effect of different doses of herb pair on the levels of AST, ALT (**A**) and LDH (**B**) in serum of rats ($\bar{x} \pm s$, n = 12, U/L).

(Compared with group K, $^{**}P < 0.01$; Compared with group M, $^{\#\#}P < 0.01$; Compared with group Y, $^{\triangle}P < 0.05$, $^{\triangle\triangle}P < 0.01$.)

3.2.3. Effects of different doses on liver morphology in rats with liver injury

According to the findings, the organization of liver cells in the K group rats was observed to be orderly, devoid of any indication of inflammatory cell infiltration, displaying a clear hepatic lobule structure, and exhibiting no signs of focal necrosis. In contrast, the M group rats demonstrated the presence of focal necrosis, steatosis, and a significant inflammatory cell infiltration in the hepatic portal area. Furthermore, each administered groups displayed an improvement in hepatocyte necrosis compared to the M group. Notably, the Y group, the D-H 1:2 middle-dose group, and the D-H 1:2 high-dose group exhibited the greatest improvement in hepatocyte necrosis (**Figure 6**).

Based on the principle of less administration and comprehensive analysis of pharmacodynamic indexes, the dosage of "Danshen-Huangqi" was determined to be 0.5 and 1.0 g/kg.

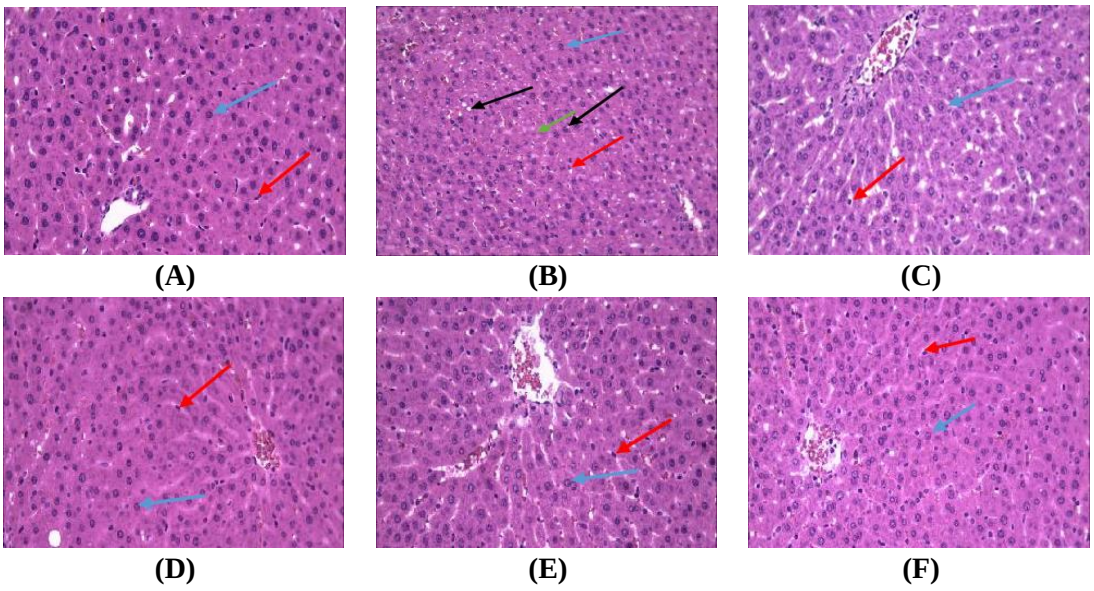

Figure 6. The effect of different doses of herb pair on liver morphology of rats (400×). (Blue arrow: liver cells; Red arrow: liver macrophages; Black arrow: hepatocyte steatosis; Green arrow: hepatocyte nuclear atrophy). **(A)**: K group; **(B)**: M group; **(C)**: Y group; **(D)**: D-H 1:2 (low) group; **(E)**: D-H 1:2 (medium) group; **(F)**: D-H 1:2 (high) group.

3.3. Effects of "Danshen-Huangqi" on CD3+, CD4+ and CD8+ T lymphocytes in peripheral blood of rats

According to the findings, there was a noticeable reduction in the population of CD3+ T lymphocytes in the peripheral blood of rats belonging to the M group when compared to the K group. Conversely, the levels of CD3+ T lymphocytes in the peripheral blood of rats across all groups were significantly elevated in contrast to the M group. Furthermore, a significant decline in CD3+ T lymphocytes in the peripheral blood of rats was observed in both the D and H groups when compared to the D-H group (**Figure 7**).

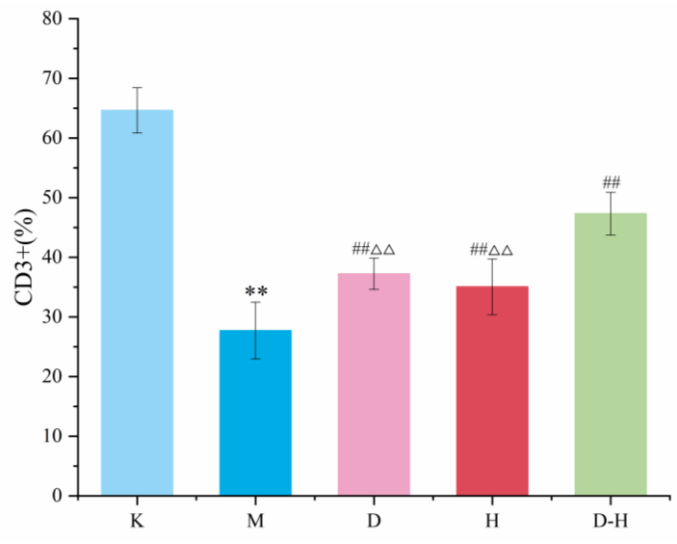

(A)

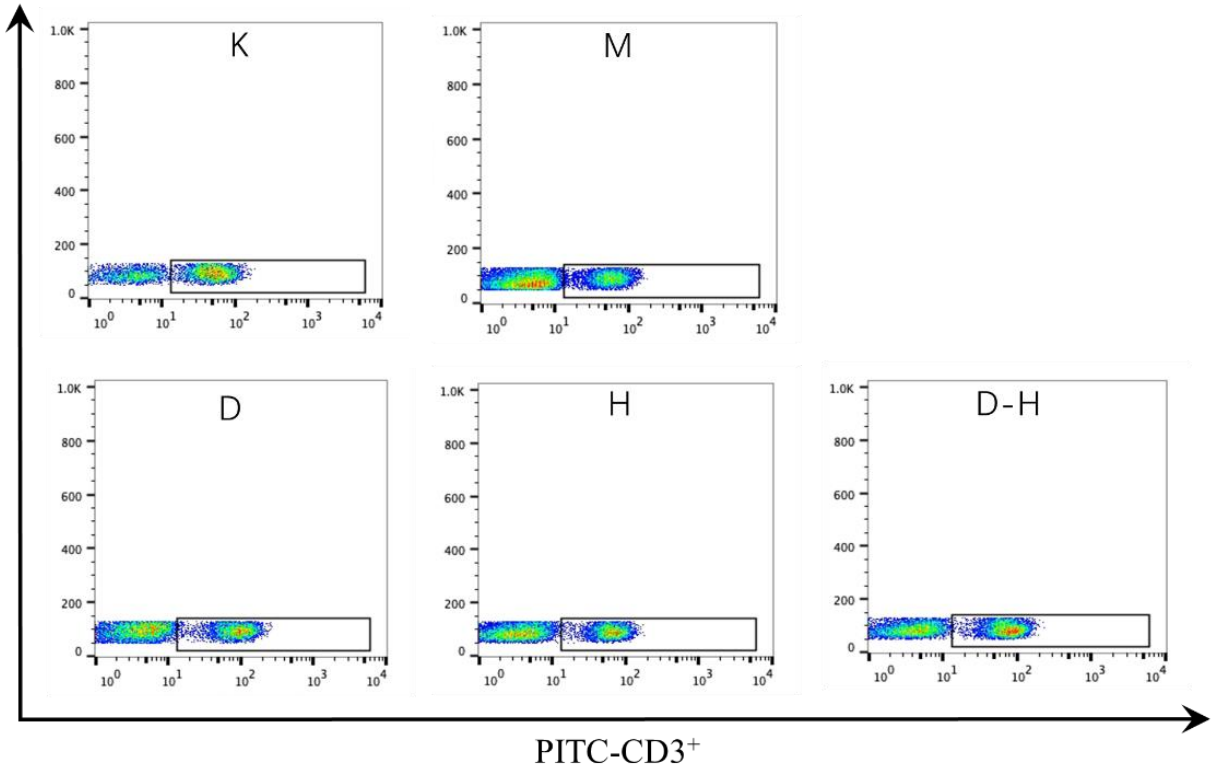

(B)

Figure 7. A: Levels of CD3+ T lymphocytes in peripheral blood of rats in different groups; B: The effect of herb pair on CD3+ T lymphocytes in peripheral blood of rats ($\bar{x} \pm s$, n = 12, %).

(Compared with group K, $^{**}P < 0.01$; Compared with group M, $^{\#\#}P < 0.01$; Compared with group D-H, $^{\triangle}P < 0.05$, $^{\triangle\triangle}P < 0.01$.)

The findings revealed a notable decrease in peripheral blood levels of CD4+ T lymphocytes, CD8+ T lymphocytes, and the CD4+/CD8+ ratio in rats assigned to the M group when compared to the K group. Conversely, a significant increase in the CD4+, CD8+ T lymphocyte ratios, and the CD4+/CD8+ ratio in peripheral blood was observed in all groups compared to the M group. Furthermore, both the D and H

groups exhibited a significant reduction in CD4+ T lymphocytes, CD8+ T lymphocytes, and the CD4+/CD8+ ratio in peripheral blood when compared to the D-H group (**Figure 8**).

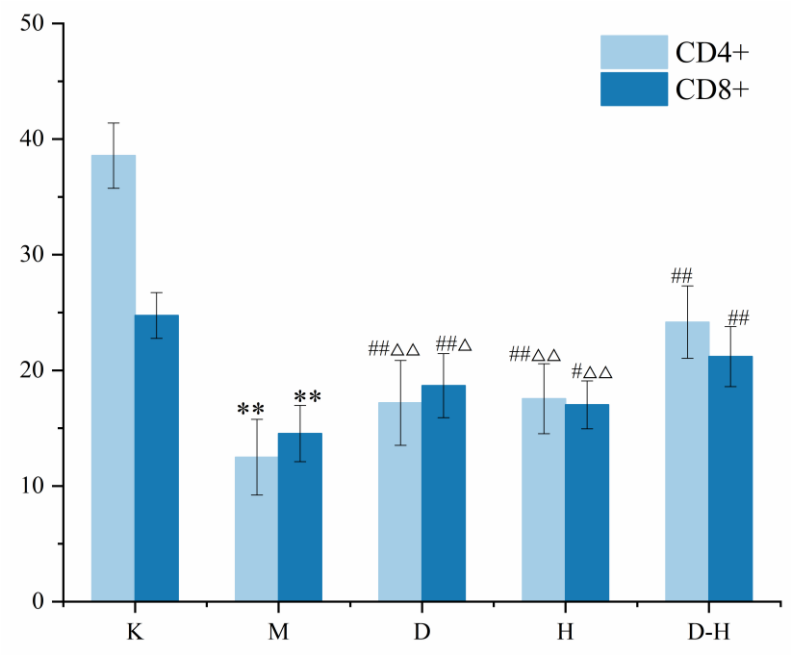

(A)

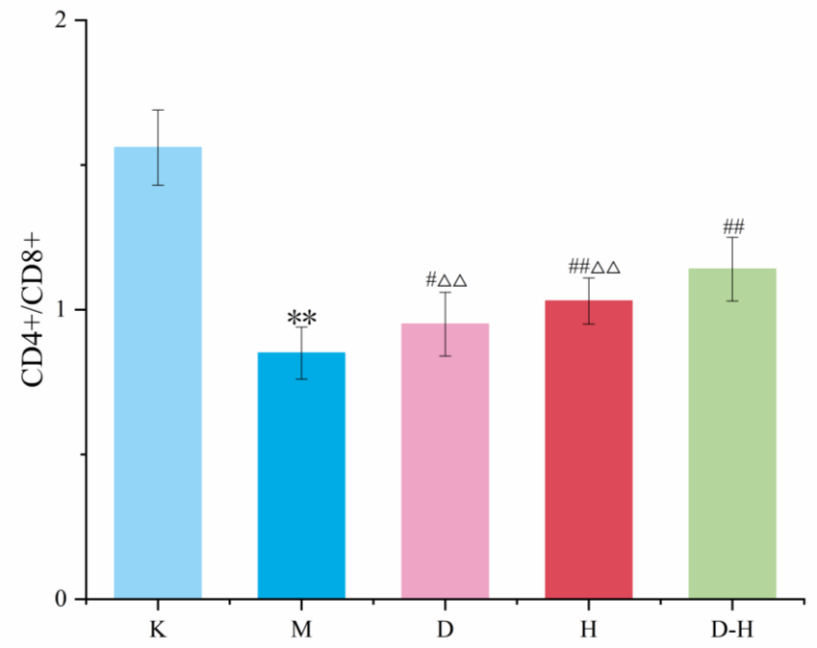

(B)

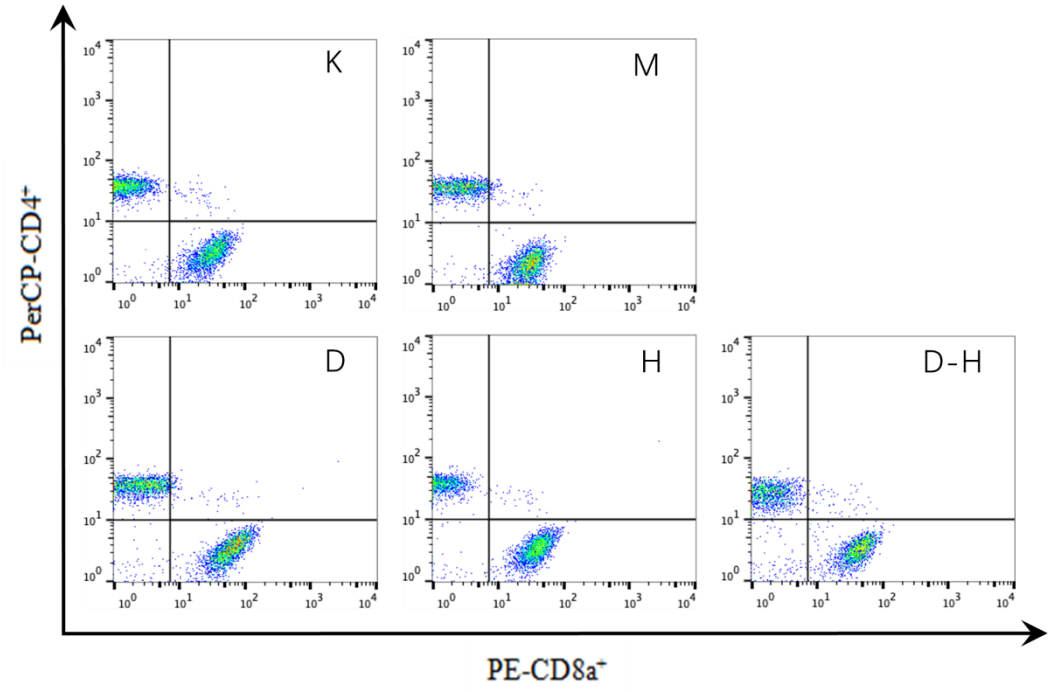

(C)

Figure 8. Levels of CD4+ , $CD8^+$ T lymphocytes **(A)** and $CD4^+/CD8^+$ T **(B)** in peripheral blood of rats in different groups. **(C)**: The effect of herb pair on $CD4^+$ and $CD8^+$ T lymphocytes in peripheral blood of rats ($\bar{x} \pm s$, n = 12).

(Compared with group K, $^{**}P < 0.01$; Compared with group M, $^{\#\#}P < 0.01$; Compared with group D-H, $^{\triangle}P < 0.05$, $^{\triangle\triangle}P < 0.01$.).

3.4. Effect of "Danshen-Huangqi" on the level of cytokines in rat serum

By analysis, the standard linear regression equation of IL-2 was $y = 0.0016x + 0.3115$ ($R^2 = 0.9958$). The standard linear regression equation of TNF-α was $y = 0.0024x + 0.0725$ ($R^2 = 0.9974$). The standard linear regression equation of IFN-γ was $y = 0.0012x + 0.1257$ ($R^2 = 0.9925$). A strong linear relationship was observed between the concentration and optical density (OD) values of IL-2, TNF-α, and IFN-γ standard samples within their respective ranges (IL-2: 31.25–2000 pg/mL, TNF-α: 15.63–1000 pg/mL, IFN-γ: 31.25–2000 pg/mL). This relationship enables accurate quantification. The findings indicated a significant increase in the levels of IL-2, TNF-α, and IFN-γ in the serum of rats in the M group compared to the K group. Furthermore, the levels of IL-2, TNF-α, and IFN-γ in the serum of rats in each administration group were significantly reduced compared to the M group. Additionally, the levels of IL-2, TNF-α, and IFN-γ in the serum of rats in the D group and H group were significantly higher than those in the D-H group (**Figure 9**).

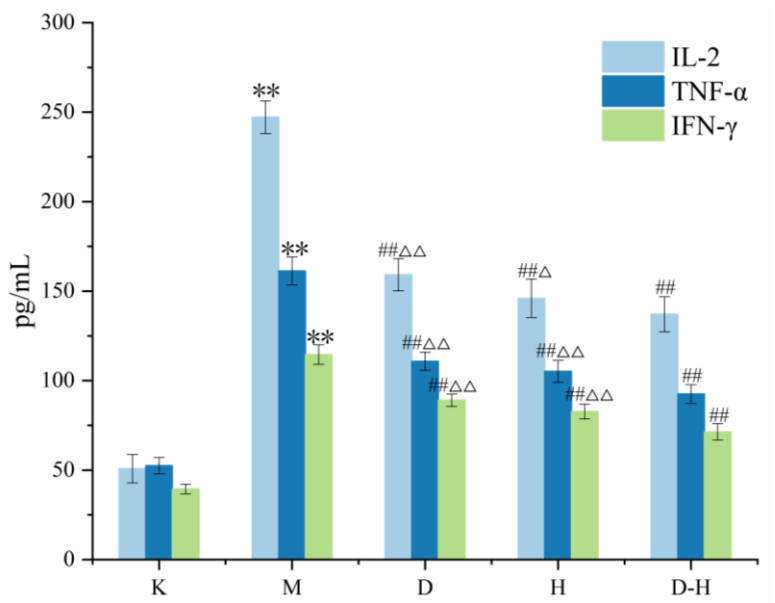

Figure 9. The effect of herb pair on IL-2, TNF-α and IFN-γ in serum of rats ($\bar{x} \pm s$, n = 12, pg/mL).

(Compared with group K, $^{**}P < 0.01$; Compared with group M, $^{\#\#}P < 0.01$; Compared with group D-H, $^{\triangle}P < 0.05$, $^{\triangle\triangle}P < 0.01$).

The linear regression equations for IL-4, IL-6, and IL-10 were as follows: y = 0.0024x + 0.0803 (R^2 = 0.9905), y = 0.0029x + 0.1141 (R^2 = 0.9938), and y = 0.0011x + 0.0842 (R^2 = 0.9915), respectively. These equations demonstrated a strong linear relationship between the concentration and OD value of standard samples within their respective ranges: 15.63–1000 pg/mL for IL-4, 12.50–800 pg/mL for IL-6, and 31.25–2000 pg/mL for IL-10. This relationship allows for accurate quantification of these cytokines. The results indicated significant differences in the serum levels of IL-4, IL-6, and IL-10 between the K group and the M group. Specifically, the levels of IL-4 and IL-10 were significantly lower in the serum of rats in the M group compared to the K group, while the level of IL-6 was significantly higher. Furthermore, when comparing the M group to each individual group, the levels of IL-4, IL-6, and IL-10 were significantly callback in the serum of rats in each group. Additionally, when comparing the D-H group to the D group and the H group, there were significant changes in the levels of IL-4, IL-6, and IL-10. The levels of IL-4 and IL-10 decreased significantly in both the D group and the H group, while the level of IL-6 increased significantly (**Figure 10**).

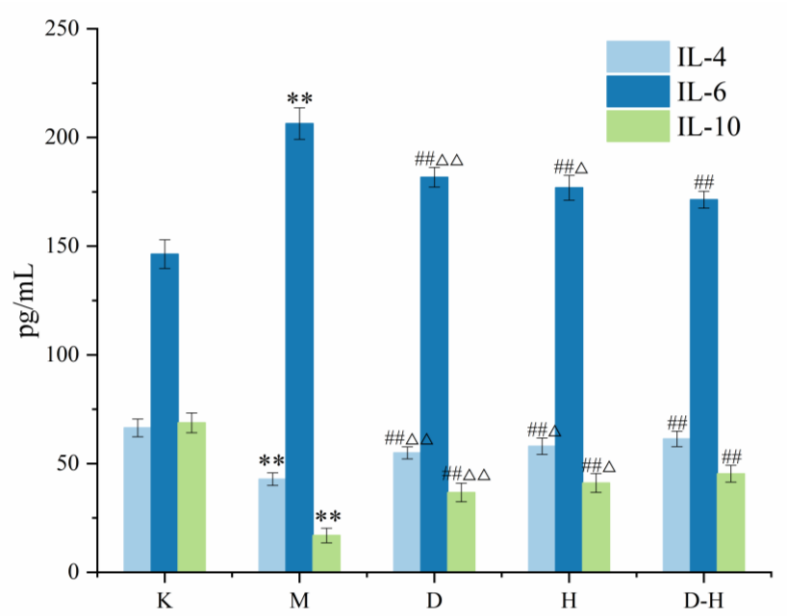

Figure 10. The effect of herb pair on IL-4, IL-6 and IL-10 in serum of rats ($\bar{x} \pm s$, n = 12, pg/mL).

(Compared with group K, $^{**}P < 0.01$; Compared with group M, $^{\#\#}P < 0.01$; Compared with group D-H, $^{\triangle}P < 0.05$, $^{\triangle\triangle}P < 0.01$).

The IL-17, IL-21, and TGF-β standard linear regression equations were as follows: $y = 0.0023x + 0.075$ ($R^2 = 0.9914$), $y = 0.0028x + 0.0383$ ($R^2 = 0.9968$), $y = 0.0003x + 0.1074$ ($R^2 = 0.9942$), respectively. The linear correlation between the concentration and OD value of IL-17 and IL-21 standard samples was highly satisfactory within the range of 15.63–1000 pg/mL, while the linear correlation between the concentration and OD value of TGF-β standard samples was also excellent within the range of 0.16–10 ng/mL. This indicates that accurate quantification can be achieved using these regression equations. The findings revealed that the serum levels of IL-17, IL-21, and TGF-β were significantly elevated in the M group compared to the K group. Additionally, when compared to the M group, the serum levels of IL-17, IL-21, and TGF-β were significantly reduced in all other groups. Furthermore, the serum levels of IL-17, IL-21, and TGF-β in the D and H groups were significantly higher than those in the D-H group (**Figures 11** and **12**).

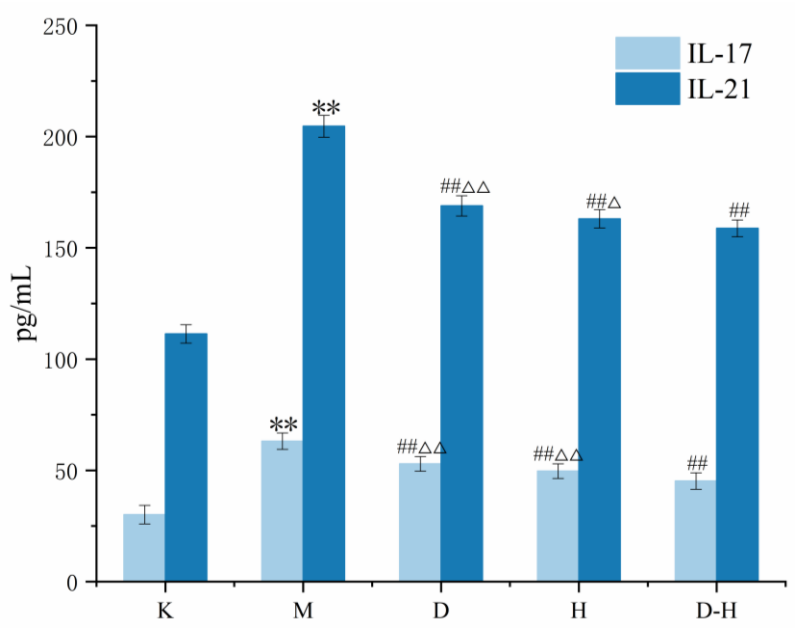

Figure 11. The effect of herb pair on IL-17 and IL-21 in serum of rats ($\bar{x} \pm s$, n = 12, pg/mL).

(Compared with group K, $^{**}P < 0.01$; Compared with group M, $^{\#\#}P < 0.01$; Compared with group D-H, $^{\triangle}P < 0.05$, $^{\triangle\triangle}P < 0.01$).

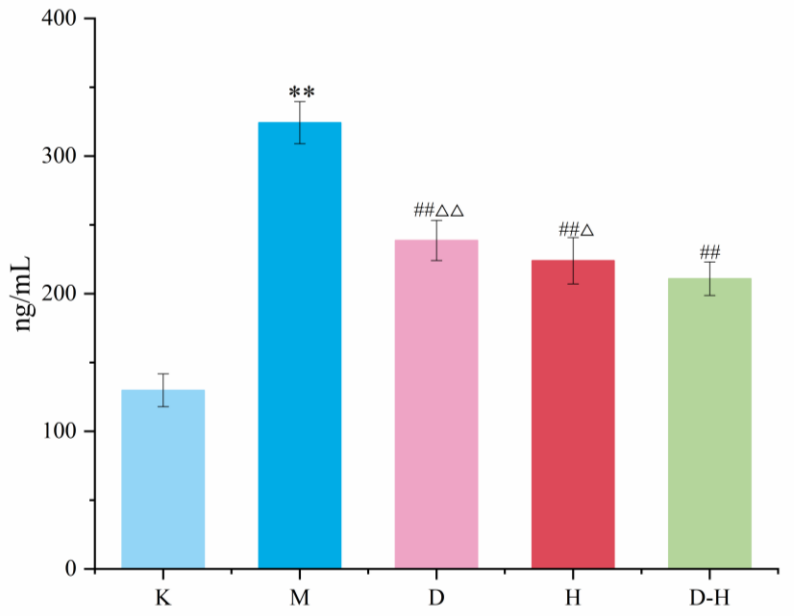

Figure 12. The effect of herb pair on TGF-β in serum of rats ($\bar{x} \pm s$, n = 12, ng/mL).

(Compared with group K, $^{**}P < 0.01$; Compared with group M, $^{\#\#}P < 0.01$; Compared with group D-H, $^{\triangle}P < 0.05$, $^{\triangle\triangle}P < 0.01$).

3.5. Detection of specific transcription factors by RT-PCR

The amplification of the double diluted cDNA template was carried out using gene primers for T-bet, GATA-3, RORγt, and Foxp3 genes, following the optimized reaction conditions. The melting curves for each gene exhibited a single peak, suggesting excellent specificity in primer amplification and the absence of any non-specific products or primer dimers. The amplification curves of each gene exhibited Ct values ranging from 20 to 40. Moreover, the observed minimal difference in the

amplification efficiency between the target gene and the reference gene. It shows that the reasonable setup of the PCR reaction system and procedure.

The findings indicated that, in comparison to the K group, there was a noteworthy increase in T-bet mRNA and T-bet/GATA-3 ratio in the liver of rats belonging to the M group, whereas GATA-3 mRNA exhibited a significant decrease. On the other hand, the liver levels of T-bet mRNA, GATA-3 mRNA, and T-bet/GATA-3 ratio were significantly callback in all groups as opposed to the M group. Similarly, in comparison to the D-H group, there was a significant increase in T-bet mRNA and T-bet/GATA-3 ratio in the liver of rats from the D group and H group, while GATA-3 mRNA displayed a significant decrease (**Figure 13**).

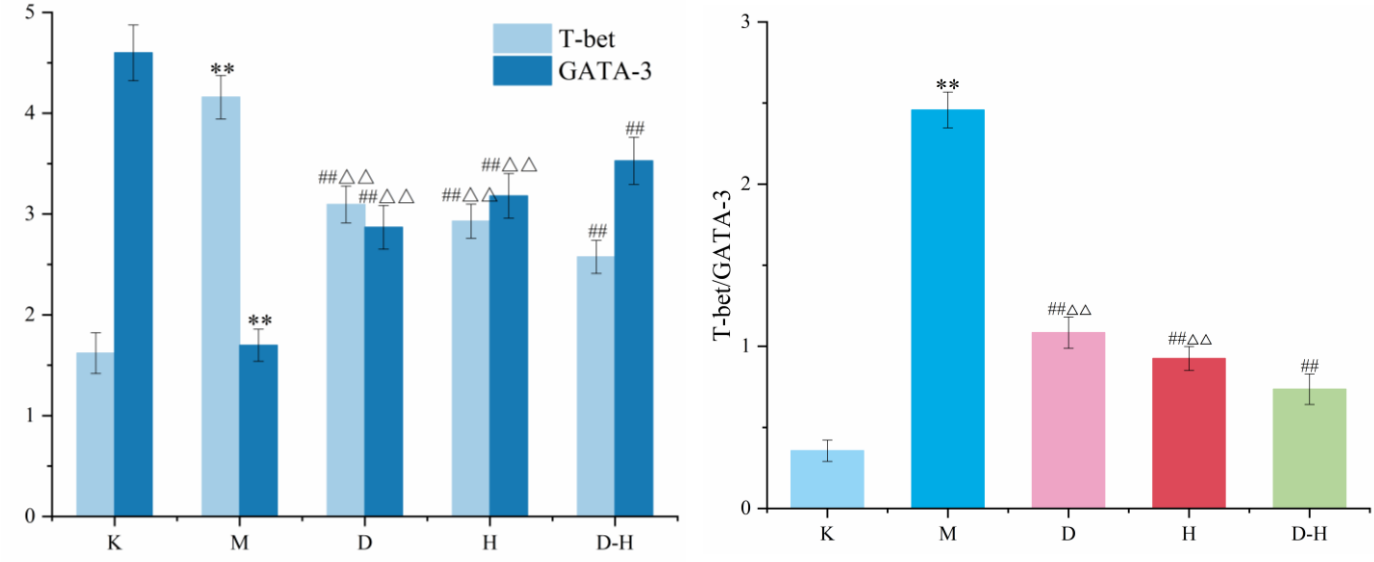

Figure 13. The effect of herb pair on T-bet , GATA-3 mRNA (**A**) and T-bet/ GATA-3 (**B**) in liver tissue of rats ($\bar{x} \pm s, n = 12$).

(Compared with group K, $^{**}P < 0.01$; Compared with group M, $^{\#\#}P < 0.01$; Compared with group D-H, $^{\triangle\triangle}P < 0.01$).

The findings indicated a significant increase in RORγt mRNA and the RORγt/Foxp3 ratio in the livers of rats in the M group compared to the K group. Additionally, there was a significant decrease in Foxp3 mRNA. Conversely, when comparing all groups to the M group, there was a significant callback observed in RORγt, Foxp3 mRNA, and the RORγt/Foxp3 ratio in the liver. Moreover, in comparison to the D-H group, both the D and H groups exhibited a significant increase in RORγt mRNA and the RORγt/Foxp3 ratio, while Foxp3 mRNA was significantly decreased in the liver of rats (**Figure 14**).

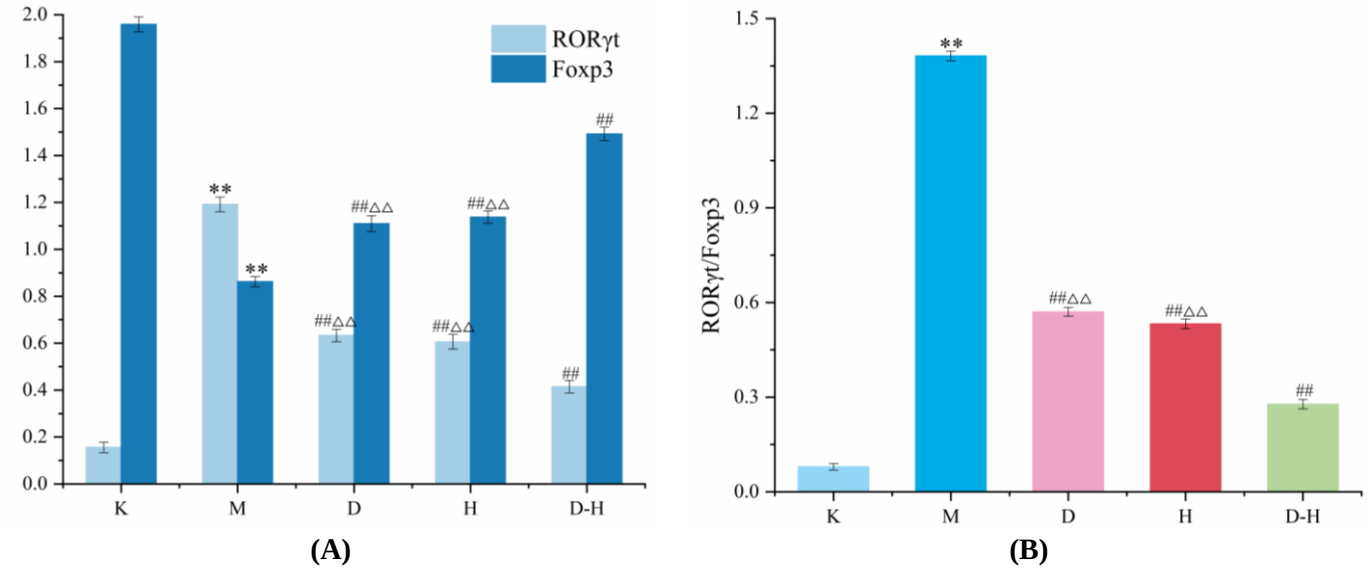

(A) **(B)**

Figure 14. The effect of herb pair on RORγt, Foxp3 mRNA **(A)** and RORγt/Foxp3 **(B)** in liver tissue of rats ($\bar{x} \pm s$, n = 12).

(Compared with group K, $^{**}P < 0.01$; Compared with group M, $^{\#\#}P < 0.01$; Compared with group D-H, $^{\triangle\triangle}P < 0.01$).

According to the findings, the levels of Fas and FasL in the rat liver were markedly elevated in the M group compared to the K group. Conversely, the liver levels of Fas and FasL were significantly reduced in all groups when compared to the M group. Notably, both the D and H groups exhibited a substantial rise in Fas and FasL levels in the liver, in comparison to the D-H group (**Figures 15**–**17**).

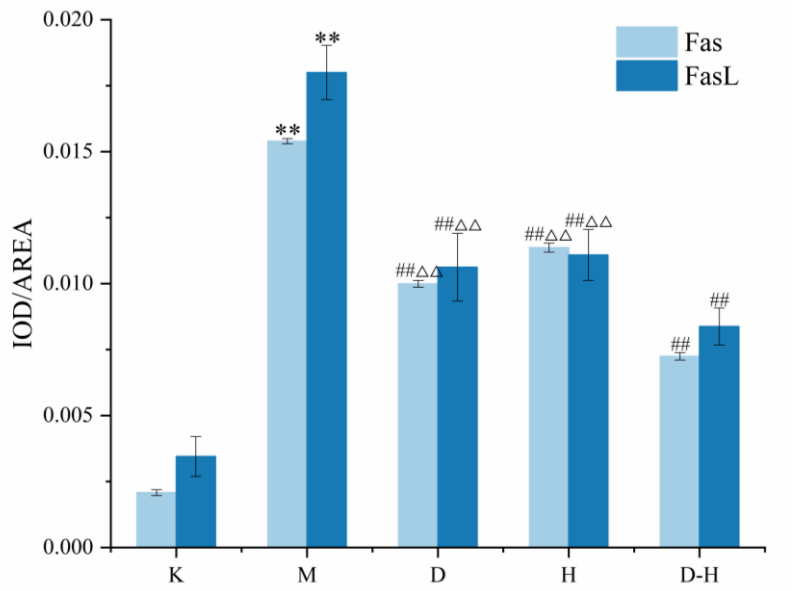

Figure 15. The effect of herb pair on Fas and FasL in liver tissue of rats ($\bar{x} \pm s$, n = 12, IOD/AREA).

(Compared with group K, $^{**}P < 0.01$; Compared with group M, $^{\#\#}P < 0.01$; Compared with group D-H, $^{\triangle\triangle}P < 0.01$.)

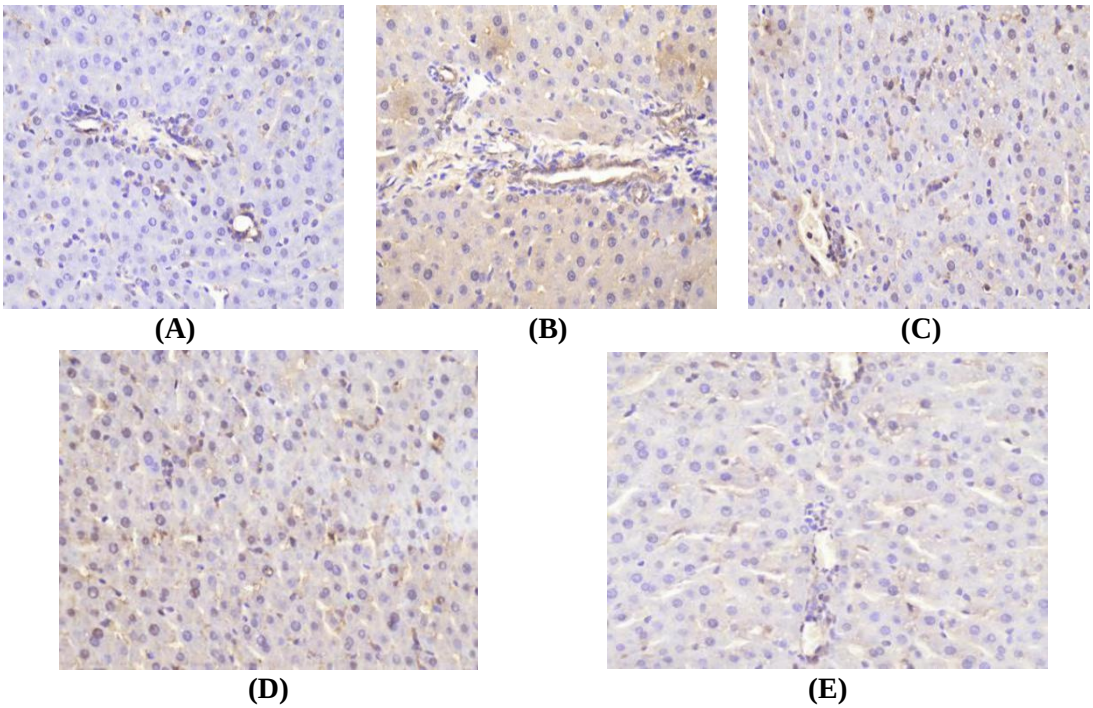

Figure 16. The effect of herb pair on Fas in liver tissue of rats (400×). **(A)**: K group; **(B)**: M group; **(C)**: D group; **(D)**: H group; **(E)**: D-H group.

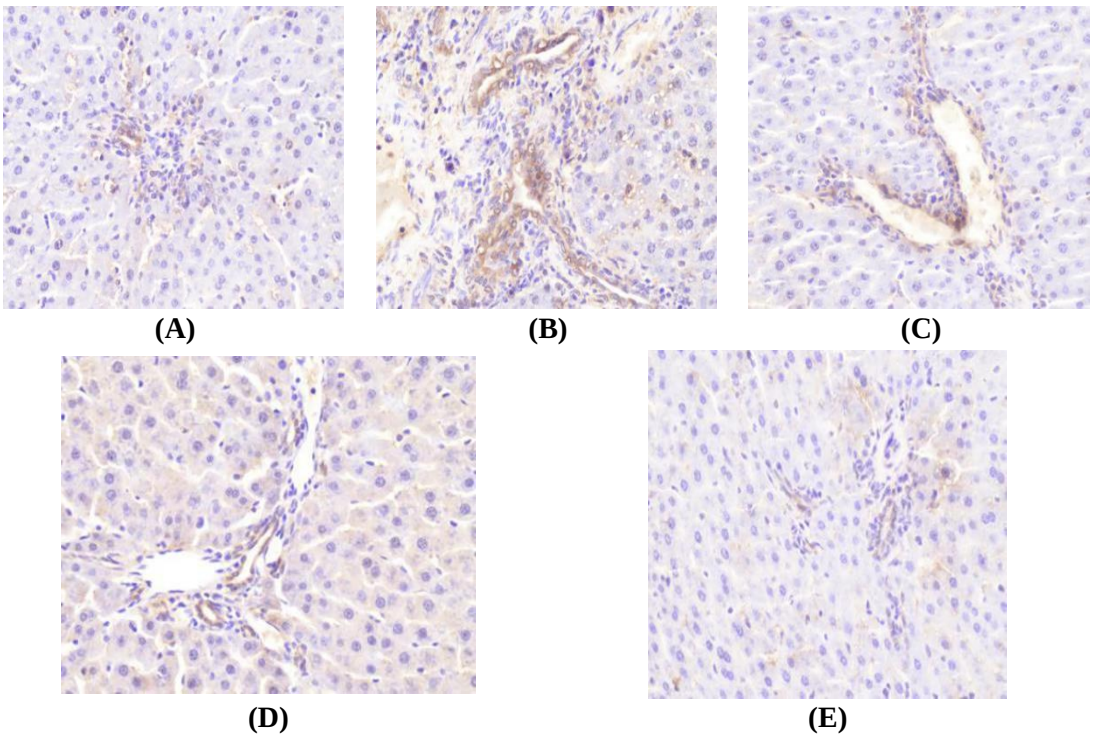

Figure 17. The effect of herb pair on FasL in liver tissue of rats (400×). **(A)**: K group; **(B)**: M group; **(C)**: D group; **(D)**: H group; **(E)**: D-H group.

The findings indicated that the liver of rats in the M group had a noteworthy increase in Bax compared to the K group, alongside a significant decrease in the ratio

of Bcl-2 and Bcl-2/Bax. Moreover, all experimental groups exhibited a significant callback in the levels of Bcl-2, Bax, and the ratio of Bcl-2/Bax in the liver of rats when compared to the M group. Additionally, Bax in the liver of rats showed a significant increase in both the D and H groups compared to the D-H group, and the ratio of Bcl-2 and Bcl-2/Bax were notably decreased (**Figures 18**–**20**).

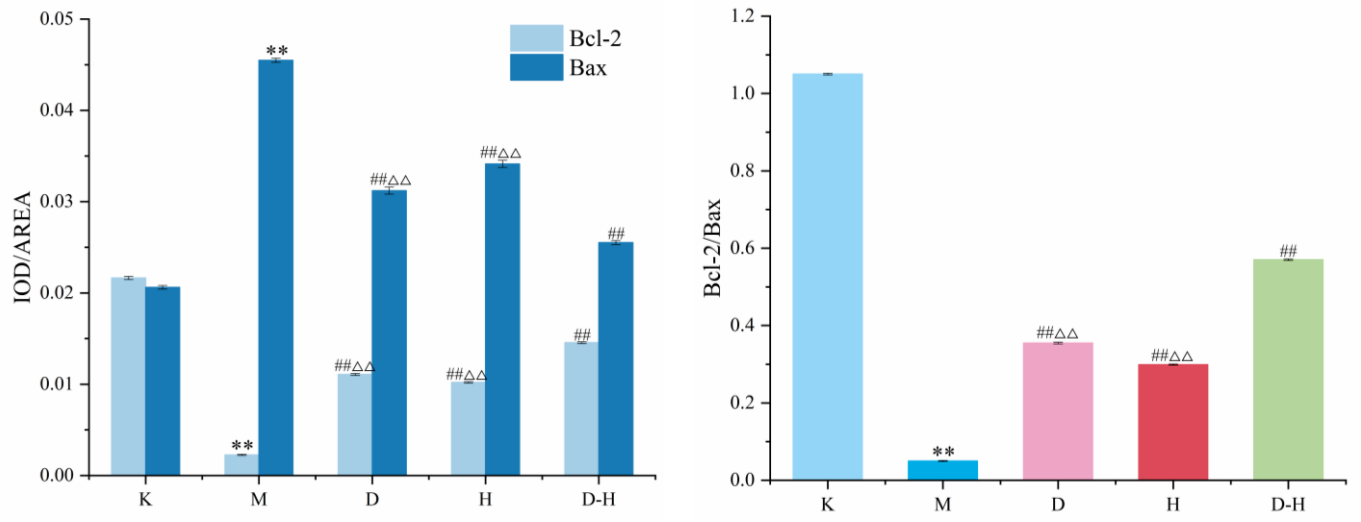

(A) **(B)**

Figure 18. The effect of herb pair on Bcl-2, Bax **(A)** and Bcl-2/Bax **(B)** in liver tissue of rats ($\bar{x} \pm s$, n = 12, IOD/AREA).

(Compared with group K, $^{**}P < 0.01$; Compared with group M, $^{\#\#}P < 0.01$; Compared with group D-H, $^{\triangle\triangle}P < 0.01$.)

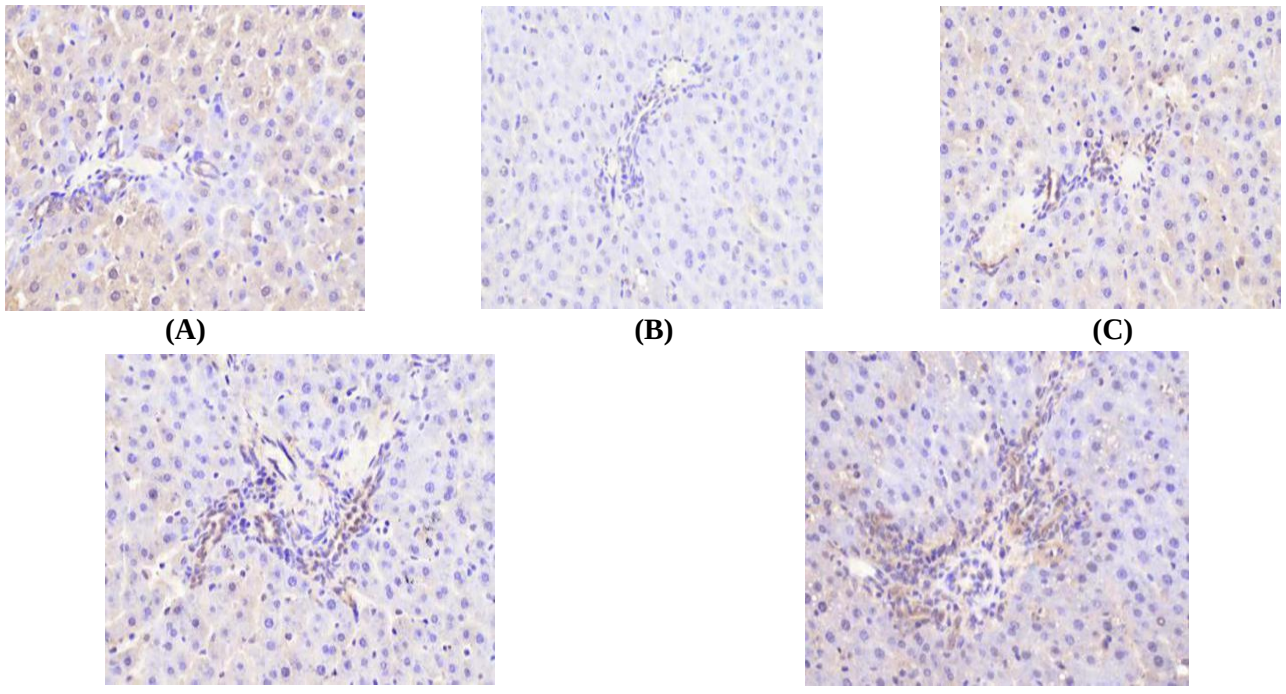

(A) **(B)** **(C)**

(D) **(E)**

Figure 19. The effect of herb pair on Bcl-2 in liver tissue of rats (400×). **(A)**: K group; **(B)**: M group; **(C)**: D group; **(D)**: H group; **(E)**: D-H group.

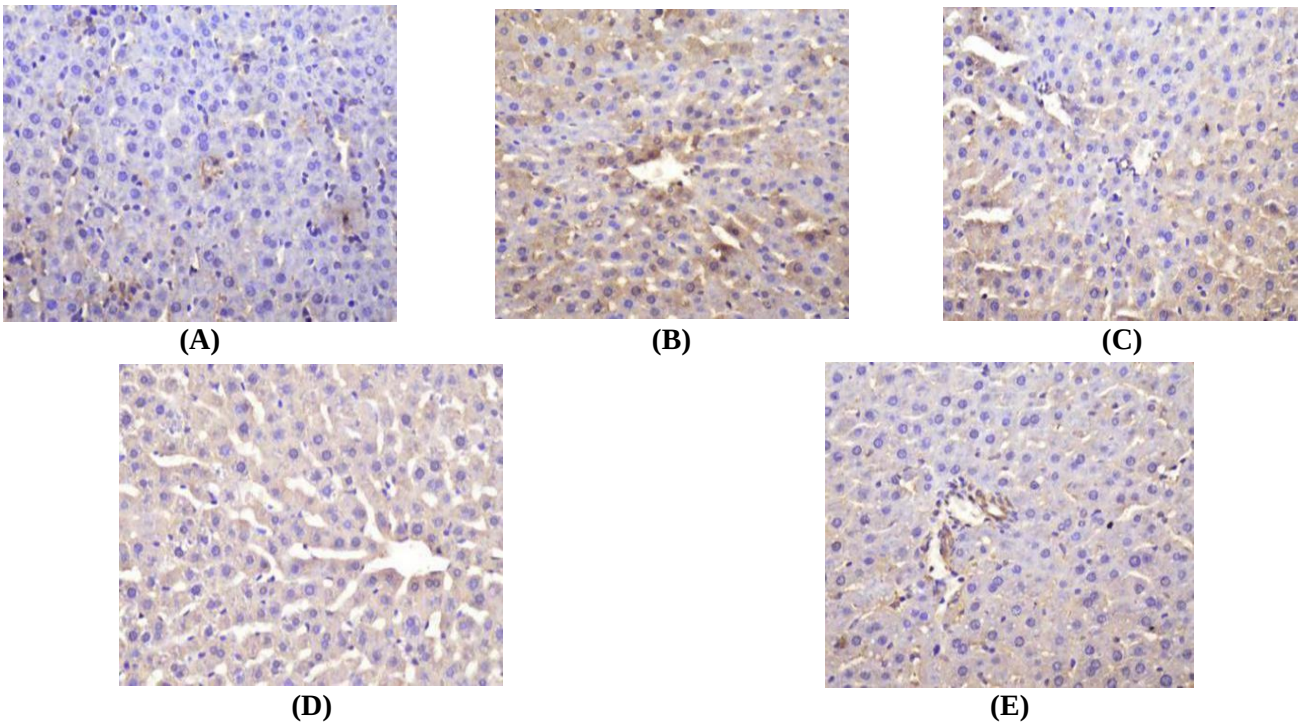

Figure 20. The effect of herb pair on Bax in liver tissue of rats (400×). **(A)**: K group; **(B)**: M group; **(C)**: D group; **(D)**: H group; **(E)**: D-H group.

4. Discussion

ConA is a kind of plant lectin, which has a strong role in promoting mitosis, inducing T cells to proliferate and differentiate, and releasing a variety of cytokines. The rat liver injury model induced by it is one of the ideal models to explore the mechanism of immune liver disease and screen liver-protecting drugs. The modeling method has the advantages of simple operation, easy repetition and high success rate of the model [21,22]. T lymphocytes exert a crucial role in both humoral and cellular immunity. In particular, CD3+ T lymphocytes encompass all mature T lymphocytes in the periphery and serve as a marker for overall cellular immunity levels [23]. Meanwhile, CD4+ T lymphocytes act as a vital cog in antiviral immune responses, promoting the proliferation and differentiation of other immune cells by releasing a wide range of cytokines [24,25]. Additionally, CD8+ T lymphocytes encompass both Tc cells and Ts cells. Under normal circumstances, the number of T lymphocytes in peripheral tissues and blood is relatively stable, and $CD4^+/CD8^+$ T lymphocytes also maintain a certain dynamic balance. If the balance is broken, the immune function of the body will be disordered. The findings of this investigation demonstrate that Danshen possesses a more potent regulatory influence over CD8+ T lymphocytes compared to Huangqi, whereas Huangqi exerts a stronger regulatory impact on CD4+ T lymphocytes than Danshen.

Distinct cellular surroundings stimulate the differentiation of Th0 cells into diverse categories of cellular subsets. Among numerous cytokines, a few essential elements including IL-2, IL-4, IL-6, IL-10, IFN-γ, and TNF-α play a pivotal role in prompting the differentiation of Th1/Th2 cellular subsets. Th1 cells mainly participate

in cellular immunity, but overexpression of Th1 cytokines can cause autoimmune diseases. Th2 cells are mainly involved in humoral immunity, and over-expressed Th2 cytokines can cause allergic asthma and parasites [26]. The body can achieve moderate disease resistance and maintain internal environmental stability only when there is a balance between Th1 cells and Th2 cells, thus preventing the occurrence of associated diseases. The findings of this investigation demonstrate that the coalescence of Danshen and Huangqi can mitigate hepatic impairment by managing the emission of Th1 and Th2 cytokines, and reinstating the equilibrium of Th1/Th2 proportion, in which Huangqi assumes a leading governing function.

The imbalance of Th17/Treg cell subsets can cause uncontrolled or excessive suppression of immune responses, leading to the occurrence of variety chronic infectious diseases and even tumors [27]. IL-17 is the main effector of Th17 cells, and its receptor is widely expressed in vivo [28]. Treg cells, a significant subset of regulatory T lymphocytes with potent immunosuppressive properties, have a vital function in the suppression of the immune response. In the body's state of immune tolerance, the differentiation of Th0 cells into Treg cells is triggered by TGF-β, leading to the prevalence of protective Treg cells. Conversely, when the body is in an immune response state, the combined action of IL-6 and TGF-β prompts the differentiation of Th0 cells into Th17 cells while inhibiting Treg cell differentiation, resulting in the dominance of pro-inflammatory Th17 cells [29]. Moreover, IL-21 possesses the capacity to prompt the differentiation of Th17 cells via the autocrine pathway, while simultaneously impeding the differentiation of Treg cells through its influence on the expression of Foxp3 [30,31]. The findings of this research reveal that the combination of Danshen and Huangqi has the capacity to modulate the release of cytokines Th17 (IL-17, IL-21) and Treg (TGF-β), and then have an auxiliary protective effect on liver injury rats, in which Huangqi plays a major regulatory role.

T-bet/GATA-3 is an exclusive transcription factor, that controls the differentiation of Th1/Th2 cell subsets from upstream, and plays a key role in maintaining the balance of Th1/Th2 cell subsets [32]. T-bet not only stimulates the expression of IFN-γ and the differentiation of Th1 cells but also suppresses the differentiation of Th2 cells. The findings of this investigation revealed that the combination of Danshen and Huangqi could potentially augment the differentiation of Th1 cells (or Th0 cells) into Th2 cells by manipulating the expression of T-bet and GATA-3, thereby sustaining the balance of Th1/Th2 cell subsets. Consequently, this exerts an adjunctive protective influence on liver-injured rats, wherein Huangqi plays a primary regulatory function. The antagonism between RORγt and Foxp3 is an important fulcrum to maintain the balance of Th17/Treg cell subsets, which are relatively independent and mutually restrictive. Once out of balance, it can lead to abnormal local or systemic immune response and induce many diseases.The study results revealed a significant rise in the expression of RORγt mRNA in Th17 cells of the rat liver following 8 h of Con A-induced modeling. Conversely, there was a significant decrease observed in the level of Foxp3 mRNA in Treg cells. These results suggest that the combination of Danshen and Huangqi may possess hepatoprotective properties by modulating the levels of transcription factors specific to Th17/Treg cell subgroups. This modulation promotes a balanced RORγt/Foxp3 ratio, thereby

regulating immune function imbalance. Notably, Huangqi exhibited superior regulatory effects compared to Danshen.

Fas, known as the "death receptor," is a transmembrane protein of type I found on the cell membrane. It is part of the superfamily of tumor necrosis factor receptors and nerve growth factor receptors, and it possesses the capacity to induce programmed cell death or apoptosis [33,34]. FasL, referred to as the "death ligand," is a type II transmembrane protein that shares structural similarity with the tumor necrosis factor superfamily [35-36]. Bax/Bcl-2 can not only form a heterodimer to play an anti-apoptotic role, but also form a homodimer to play a pro-apoptotic role [37-39]. When the relative expression of Bax is higher than that of Bcl-2, homodimers can be formed and the expression of Bax can be increased, thereby promoting apoptosis. When the relative expression of Bax is lower than that of Bcl-2, it can form heterodimers and increase the expression of Bcl-2, thus inhibiting apoptosis. The research findings indicated that the "Danshen-Huangqi" combination exhibited a notable ability to suppress abnormal hepatocyte apoptosis by reducing the levels of Bax, Fas, FasL and increasing the expression of Bcl-2. Notably, Danshen demonstrated a superior regulatory effect compared to Huangqi. The protective impact of the "Danshen-Huangqi" combination against ConA-induced liver injury is visually depicted in **Figure 21**.

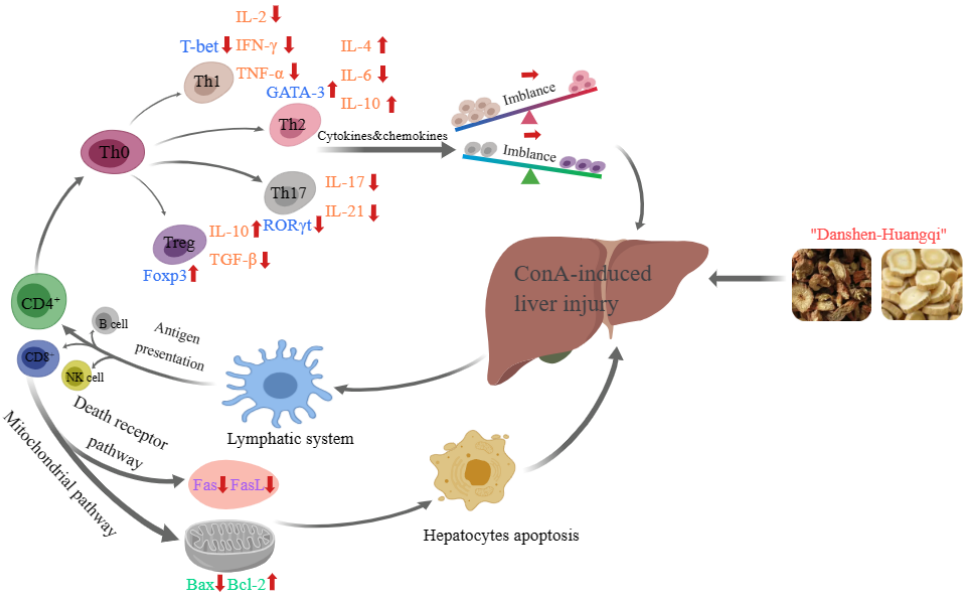

Figure 21. Protective effects of "Danshen-Huangqi" on ConA-induced liver injury.

5. Conclusion

The combination of "Danshen-Huangqi" has a good preventive and therapeutic effect on Con A-induced liver injury, especially when administering the drug pair at 0.5g/kg, 1.0g/kg dosages. "Danshen-Huangqi" can regulate T lymphocyte subsets in two directions, which can not only correct the imbalance of Th1/Th2 and Th17/Treg cell subsets by regulating the secretion of Th1, Th2, Th17, Treg cytokines and specific transcription factors. It can also inhibit the abnormal apoptosis of hepatic lymphocytes by regulating the expression of apoptosis-related genes in the death receptor pathway

(Fas, FasL) and mitochondrial pathway (Bcl-2, Bax) in the liver of rats with liver injury. Our research provides a valuable basis for the clinical application of "Danshen-Huangqi" to protect liver injury, and also presents a promising avenue for the development and application of health care products for preventing liver injury in the times to come.

Author contributions: Investigation, TG and JF; methodology, TG and YW; visualization, TG; writing—original draft, TG; writing—review & editing, TG and JF; validation, data curation, JF; conceptualization, investigation, resources, FG; supervision, FG and YW; project administration, funding acquisition, YW. All authors have read and agreed to the published version of the manuscript.

Funding: This work was supported by the National Natural Science Foundation of China (grant number 82074025); and Heilongjiang University of Traditional Chinese Medicine Health Industry Special Project (grant number 2018jkcy03).

Data availability: Data will be made available on request.

Ethical approval: The animal study protocol was approved by the Animal Ethics Committee of Heilongjiang University of Chinese Medicine which adhered to the guidelines established by the National Institute of Health and Nutrition for the Care and Use of Laboratory Animals (Approval number: DXLL2019061601).

Conflict of interest: The authors declare no conflict of interest.

References

1. Li N, Li B, Zhang J, et al, Protective effect of phenolic acids from Chebulae Fructus immaturus on carbon tetrachloride induced acute liver injury via suppressing oxidative stress, inflammation and apoptosis in mouse, Nat Prod Res. 34 (2020) 3249-3252, https://doi.org/10.1080/14786419.2018.1553174.
2. Ren, M., Lu, C., Zhou, M., Jiang, X., Li, X., & Liu, N. (2024). The intersection of virus infection and liver disease: A comprehensive review of pathogenesis, diagnosis, and treatment. WIREs Mechanisms of Disease, 16(3), e1640. https://doi.org/10.1002/wsbm.1640
3. Devarbhavi H, Asrani SK, Arab JP, Nartey YA, Pose E, Kamath PS, Global burden of liver disease: 2023 update, J Hepatol. 79 (2023) 516-537, https://doi.org/10.1016/j.jhep.2023.03.017.
4. Hao, J., Sun, W., & Xu, H. (2022). Pathogenesis of concanavalin A induced autoimmune hepatitis in mice. International Immunopharmacology, 102, 108411. https://doi.org/10.1016/j.intimp.2021.108411
5. Wu S, Sa R, Gu Z, et al, The Protective Effect of Aesculus hippocastanum (Venoplant®) Against Concanavalin A-Induced Liver Injury, Pharmacology. 104 (2019) 196-206, https://doi.org/10.1159/000501258.
6. Wang Y, Chen J, Chen Y, Wu XT, Improvement of nonalcoholic fatty liver disease in ALT at ⩾12 months after Roux-en-Y gastric bypass and sleeve gastrectomy, no effect in ALT and AST at <12 months after SG and in AST at >12 and ⩽24 months after RYGB, Surg Obes Relat Dis. 16 (2020) 447-450, https://doi.org/10.1016/j.soard.2019.10.030.
7. Hwang W, Lee J, Pathophysiologic Implications of Cytokines Secretion during Liver Transplantation Surgery, Int J Med Sci. 15 (2018) 1737-1745, https://doi.org/10.7150/ijms.28382.
8. Wang L, Du H, Liu Y, Wang L, Ma X, Zhang W, Chinese medicine bu xu 24u ayu recipe for the regulation of treg/th17 ratio imbalance in autoimmune hepatitis, Evid Based Complement Alternat Med. 2015 (2015) 461294, https://doi.org/10.1155/2015/461294.
9. Song Y, Wu X, Yang D, et al, Protective Effect of Andrographolide on Alleviating Chronic Alcoholic Liver Disease in Mice by Inhibiting Nuclear Factor Kappa B and Tumor Necrosis Factor Alpha Activation, J Med Food. 23 (2020) 409-415, https://doi.org/10.1089/jmf.2019.4471.

10. Elshal M, Abu-Elsaad N, El-Karef A, Ibrahim T, Retinoic acid modulates IL-4, IL-10 and MCP-1 pathways in immune mediated hepatitis and interrupts CD4+ T cells infiltration, Int Immunopharmacol. 75 (2019) 105808, https://doi.org/10.1016/j.intimp.2019.105808.
11. Tian X, Liu Y, Liu X, Gao S, Sun X, Glycyrrhizic acid ammonium salt alleviates Concanavalin A-induced immunological liver injury in mice through the regulation of the balance of immune cells and the inhibition of hepatocyte apoptosis, Biomed Pharmacother. 120 (2019) 109481, https://doi.org/10.1016/j.biopha.2019.109481.
12. Wang K, Molecular mechanisms of hepatic apoptosis regulated by nuclear factors, Cell Signal. 27 (2015) 729-738, https://doi.org/10.1016/j.cellsig.2014.11.038.
13. Alhusaini AM, Faddah LM, Hasan IH, et al, Vitamin C and Turmeric Attenuate Bax and Bcl-2 Proteins' Expressions and DNA Damage in Lead Acetate-Induced Liver Injury, Dose Response. 17 (2019) 1559325819885782. https://doi.org/10.1177/1559325819885782.
14. Zhou Y, Chen K, He L, et al, The Protective Effect of Resveratrol on Concanavalin-A-Induced Acute Hepatic Injury in Mice, Gastroenterol Res Pract. 2015 (2015) 506390, https://doi.org/10.1155/2015/506390.
15. Fernandes P, O'Donnell C, Lyons C, et al, Intestinal expression of Fas and Fas ligand is upregulated by bacterial signaling through TLR4 and TLR5, with activation of Fas modulating intestinal TLR-mediated inflammation, J Immunol. 193 (2014) 6103-6113, https://doi.org/10.4049/jimmunol.1303083.
16. Heymann F, Hamesch K, Weiskirchen R, Tacke F, The concanavalin A model of acute hepatitis in mice, Lab Anim. 49 (2015) 12-20, https://doi.org/10.1177/0023677215572841.
17. Yue S, Hu B, Wang Z, et al, Salvia miltiorrhiza compounds protect the liver from acute injury by regulation of p38 and NFκB signaling in Kupffer cells, Pharm Biol. 52 (2014) 1278-1285, https://doi.org/10.3109/13880209.2014.889720.
18. Shi MJ, Dong BS, Yang WN, Su SB, Zhang H, Preventive and therapeutic role of Tanshinone ⅡA in hepatology, Biomed Pharmacother. 112 (2019) 108676, https://doi.org/10.1016/j.biopha.2019.108676.
19. Alam P, Parvez MK, Arbab AH, Al-Dosari MS, Quantitative analysis of rutin, quercetin, naringenin, and gallic acid by validated RP- and NP-HPTLC methods for quality control of anti-HBV active extract of Guiera senegalensis, Pharm Biol. 55 (2017) 1317-1323, https://doi.org/10.1080/13880209.2017.1300175.
20. Chen LY, Sun TT, Zhu D, et al, Protective Mechanism of Astragalus Ⅳ Combined with Salvianolic Acid B on Hepatocyte (HHL － 5) Peroxidation Injury, Liaoning Journal of Traditional Chinese Medicine, 46 (2019) 1488-1490+1569, http://dx.doi.org/10.13192/j.issn.1000-1719.2019.07.042.
21. Xie D, Zhou P, Liu L, et al, Protective Effect of Astragaloside IV on Hepatic Injury Induced by Iron Overload, Biomed Res Int. 2019 (2019) 3103946, https://doi.org/10.1155/2019/3103946.
22. Jiang Z, Zheng L, Magnesium isoglycyrrhizinate protects against concanavalin A-induced immunological liver injury in a mouse model, Rev Rom Med Lab. 27 (2019) 281-290, https://doi.org/10.2478/rrlm-2019-0026.
23. Getachew Y, Cusimano FA, James LP, Thiele DL, The role of intrahepatic CD3+/CD4-/CD8- double negative T (DN T) cells in enhanced acetaminophen toxicity, Toxicol Appl Pharmacol. 280 (2014) 264-271, https://doi.org/10.1016/j.taap.2014.08.017.
24. Su L, Wu Z, Chi Y, et al, Mesenteric lymph node CD4+ T lymphocytes migrate to liver and contribute to non-alcoholic fatty liver disease, Cell Immunol. 337 (2019) 33-41, https://doi.org/10.1016/j.cellimm.2019.01.005.
25. Rao J, Cheng F, Yang S, Zhai Y, Lu L, Ag-specific CD4 T cells promote innate immune responses in liver ischemia reperfusion injury, Cell Mol Immunol. 16 (2019) 98-100, https://doi.org/10.1038/s41423-018-0051-x.
26. Liu HM, Han YZ, Guo YM, et al, The protection effects of Liuweiwuling tablets against concanavalin A-induced acute immunological liver injury in mice, Chin Pharmacol Bull. 33 (2017) 133-140, https://doi.org/10.3969/j.issn.1001-1978.2017.01.023.
27. Yang C, Cui F, Chen LM, Gong XY, Qin B, Correlation between Th17 and nTreg cell frequencies and the stages of progression in chronic hepatitis B, Mol Med Rep. 13 (2016) 853-859, https://doi.org/10.3892/mmr.2015.4618.
28. Akberova D, Kiassov AP, Abdulganieva D, Serum Cytokine Levels and Their Relation to Clinical Features in Patients with Autoimmune Liver Diseases, J Immunol Res. 2017 (2017) 9829436, https://doi.org/10.1155/2017/9829436.
29. Gong Y, Liu H, Tao L, Cajanonic acid A regulates the ratio of Th17/Treg via inhibition of expression of IL-6 and TGF-β in insulin-resistant HepG2 cells [retracted in: Biosci Rep. 2022 Jan 28;42(1):], Biosci Rep. 39 (2019) BSR20181716, https://doi.org/10.1042/BSR20181716.

30. Cho J, Kim S, Yang DH, et al, Mucosal Immunity Related to FOXP3+ Regulatory T Cells, Th17 Cells and Cytokines in Pediatric Inflammatory Bowel Disease, J Korean Med Sci. 33 (2018) e336, https://doi.org/10.3346/jkms.2018.33.e336.
31. Tan Y, Chen W, Liu C, Zheng X, Guo A, Long J, Effect of IL-21 on the Balance of Th17 Cells/Treg Cells in the Pathogenesis of Graves' Disease, Endocr Res. 44 (2019) 138-147, https://doi.org/10.1080/07435800.2019.1600535.
32. Zhu K, Ye J, Wu M, Cheng H, Expression of Th1 and Th2 cytokine-associated transcription factors, T-bet and GATA-3, in peripheral blood mononuclear cells and skin lesions of patients with psoriasis vulgaris, Arch Dermatol Res. 302 (2010) 517-523, https://doi.org/10.1007/s00403-010-1048-1.
33. Cubero FJ, Woitok MM, Zoubek ME, de Bruin A, Hatting M, Trautwein C, Disruption of the FasL/Fas axis protects against inflammation-derived tumorigenesis in chronic liver disease, Cell Death Dis. 10 (2019) 115, https://doi.org/10.1038/s41419-019-1391-x.
34. Zhu H, Berkova Z, Mathur R, et al, HuR Suppresses Fas Expression and Correlates with Patient Outcome in Liver Cancer, Mol Cancer Res. 13 (2015) 809-818, https://doi.org/10.1158/1541-7786.MCR-14-0241.
35. Berger RML, Weck JM, Kempe SM, et al. Nanoscale FasL Organization on DNA Origami to Decipher Apoptosis Signal Activation in Cells. Small. 2021;17(26):e2101678. Doi:10.1002/smll.202101678
36. Abou Shousha S, Baheeg S, Ghoneim H, Zoheir M, Hemida M, Shahine Y. The effect of Fas/FasL pathway blocking on apoptosis and stemness within breast cancer tumor microenvironment (preclinical study). Breast Dis. 2023;42(1):163-176. Doi:10.3233/BD-220077
37. Qian, S., Wei, Z., Yang, W., Huang, J., Yang, Y., & Wang, J. (2022). The role of BCL-2 family proteins in regulating apoptosis and cancer therapy. Frontiers in oncology, 12, 985363. https://doi.org/10.3389/fonc.2022.985363
38. Gitego, N., Agianian, B., Mak, O.W. et al. Chemical modulation of cytosolic BAX homodimer potentiates BAX activation and apoptosis. Nat Commun 14, 8381 (2023). https://doi.org/10.1038/s41467-023-44084-3
39. Kaloni D, Diepstraten ST, Strasser A, Kelly GL. BCL-2 protein family: attractive targets for cancer therapy. Apoptosis. 2023;28(1-2):20-38. doi:10.1007/s10495-022-01780-7